Accepted Manuscript

Petroleum Geoscience

Quantification of solubility trapping in natural and engineered CO_2 reservoirs

Rory Leslie, Andrew J. Cavanagh, R. Stuart Haszeldine, Gareth Johnson & Stuart M. V. Gilfillan

DOI: https://doi.org/10.1144/petgeo2020-120

To access the most recent version of this article, please click the DOI URL in the line above. When citing this article please include the above DOI.

This article is part of the Geoscience for CO_2 storage collection available at: https://www.lyellcollection.org/cc/geoscience-for-co2-storage

Received 30 October 2020
Revised 11 June 2021
Accepted 21 June 2021

Supplementary material at https://doi.org/10.6084/m9.figshare.c.5476199

Quantification of Solubility Trapping in Natural and Engineered CO_2 Reservoirs

Rory Leslie[1]*, Andrew J. Cavanagh[1], R. Stuart Haszeldine[1,2], Gareth Johnson[3] and Stuart M.V. Gilfillan[1]

[1] School of GeoSciences, Grant Institute, University of Edinburgh, Edinburgh, EH9 3FE, UK
[2] SCCS, High School Yards, Infirmary Street, Edinburgh, EH1 1LZ, Scotland
[3] Department of Civil and Environmental Engineering, University of Strathclyde, Glasgow, G1 1XZ, UK

* Correspondence address: rory.leslie@ed.ac.uk

Solubility Trapping Nat. & Eng. CO_2 Res.

Abstract: Secure retention of CO_2 in geological reservoirs is essential for effective storage. Solubility trapping, the dissolution of CO_2 into formation water, is a major sink on geological timescales in natural CO_2 reservoirs. Observations during CO_2 injection, combined with models of CO_2 reservoirs, indicate the immediate onset of solubility trapping. There is uncertainty regarding the evolution of dissolution rates between the observable engineered timescale of years and decades, to the >10 kyr state represented by natural CO_2 reservoirs. A small number of studies have constrained dissolution rates within natural analogues. The studies show that solubility trapping is the principal storage mechanism after structural trapping, removing 10–50% of CO_2 across whole reservoirs. Natural analogues, engineered reservoirs and model studies produce a wide range of estimates on the fraction of CO_2 dissolved and the dissolution rate. Analogue and engineered reservoirs do not show the high fractions of dissolved CO_2 seen in several models. Evidence from natural analogues supports a model of most dissolution occurring during emplacement and migration, before the establishment of a stable gas-water contact. A rapid decline in CO_2 dissolution rate over time suggests that analogue reservoirs are in dissolution equilibrium for most of the CO_2 residence time.

Supplementary material: [All data used in this paper are contained in the supplementary information spreadsheet included with the submission. A doi and permanent url do not exist. Therefore, we wish to use the GSL figshare portal]

CO_2 trapping mechanisms are physical and chemical processes that prevent CO_2 from migrating out of a reservoir. For CO_2 capture and storage (CCS), trapping is the key to secure and long-term sequestration of CO_2 (Alcalde *et al.* 2018; Miocic *et al.* 2018). Structural and stratigraphic trapping beneath a seal, such as a shale caprock, and residual trapping in the reservoir pores through which the CO_2 migrates, are essential components of the initial storage. Depending on storage depth, injected CO_2 exists as a gas, liquid or supercritical phase. We use the term ‘free-phase’ to refer to CO_2 in the gas, liquid or supercritical phases to differentiate it from aqueous CO_2 dissolved in formation water. CO_2 dissolution, also called solubility trapping, can remove free-phase CO_2 over time (Ajayi *et al.* 2019). Formation water has the potential to store up to 50 kg/m^3 of dissolved CO_2 when fully saturated at reservoir conditions of 37°C and 100 kbar. The 37°C and 100 kbar reservoir conditions approximate the Utsira Formation at the Sleipner storage reservoir and are typical of offshore sites considered for saline aquifer storage (Steel *et al*. 2016). CO_2-saturated formation water is slightly denser than ambient formation water and sinks in the reservoir. Naturally occurring CO_2 reservoirs can be used as analogues for understanding processes, such as solubility trapping, over geological timescales (Allis *et al*. 2001; Haszeldine *et al*. 2005). Solubility trapping is significant in these analogue reservoirs (Gilfillan *et al*. 2009; Zhou *et al*. 2012). In the widely cited Bravo Dome CO_2 field (Sathaye *et al*. 2014; Zwahlen *et al*. 2017) solubility trapping has removed between 10–50% of the 1600–1800 million metric tonnes (Mt) of CO_2 originally emplaced.

The physics and chemistry of CO_2 dissolution in storage reservoirs are well understood. Increased pressure increases solubility; while increased temperature and salinity reduce solubility (Spycher & Pruess 2005; Pruess & Spycher 2007; Riaz & Cinar 2014; Jacob & Saylor 2016). Pre-injection formation water may contain dissolved CO_2, in equilibrium with carbonate minerals. Injection of free-phase CO_2 increases the partial pressure of CO_2 in the reservoir. The increased fugacity of the CO_2 would, according to Henry’s Law, cause dissolution of the CO_2 into the formation water (Majer *et al.* 2008). Dissolution will stop when a new equilibrium is reached. Knowledge of the formation water volume, salinity, initial CO_2 saturation, reservoir pressure and temperature allows for a good approximation of the potential maximum mass of dissolved CO_2.

Free-phase CO_2 and water are immiscible (Newmark *et al*. 2010). At the storage reservoir scale (>1 km), the CO_2 dissolution rate is effectively controlled by the surface-area of the free-phase CO_2 plume and by CO_2 mobility, which allows contact with formation water. Capillary action, viscous flow, pressure and gravity control the migration of the CO_2 plume in the reservoir. Molecular diffusion of CO_2 within the formation water causes very low rates of dissolution (Pruess & Nordbotten 2011) but can persist after emplacement and stabilisation of the CO_2 plume. Diffusion may be the main process facilitating CO_2 dissolution over geological timescales in reservoirs where density-driven convection does not occur. If the Rayleigh number, primarily controlled by reservoir permeability, is sufficiently high, then density-driven convection may initiate at the front of the migrating CO_2 plume. The convection is driven by the increased density of CO_2-saturated formation water relative to ambient formation water. Convection enhances dissolution rates by circulating more CO_2-saturated formation water away from the plume and less CO_2-saturated formation water towards the plume (Ajayi *et al.* 2019). Since convection accelerates the volume of formation water contacted, it increases the rate of CO_2 dissolution (Pruess & Nordbotten 2011). Convection may continue after stabilisation of the CO_2 plume and enhance long-term dissolution rates compared to diffusion-only scenarios. In a closed system, convection will still result in the same mass of CO_2 dissolved. In reservoirs with aquifer flow (advection), the total mass and rate of CO_2 dissolution will be higher, since the total volume and rate of formation water contacting the CO_2 is higher.

The total mass and rates of CO_2 dissolution in engineered sites are debated. Estimates of dissolution can vary widely due to the large number of site-specific variables (e.g. permeability, anisotropy, heterogeneity) and fluid dynamics (diffusion, convection, and advection) which are difficult to accurately quantify. Some authors have attempted universal algorithmic formulations that capture the expected behaviour (e.g. Martinez & Hesse 2016), while others have demonstrated the adaptability of numerical reservoir simulators to estimate outcomes for specific case studies (e.g. Pickup *et al*. 2011).

In natural CO_2 reservoirs, large volumes of CO_2 have been trapped in sedimentary rocks on geological timescales. Commonly cited examples of commercially exploited CO_2 accumulations from the Colorado Plateau, Rocky Mountains and Gulf Coast regions of the USA have undergone detailed geochemical studies (Allis *et al*. 2001, Gilfillan *et al*. 2008; Gilfillan *et al*. 2009; Zhou *et al*. 2012). Results from geochemical studies can help inform modelling studies of CO_2 dissolution and provide a comparison with measurements from operational CCS sites to better calibrate predictive models of long-term solubility trapping. Here, we focus on using natural analogues to complement studies of solubility trapping using modelling and observations from engineered CO_2 reservoirs. We examine both the total dissolved CO_2 mass and dissolution rate with a focus on timescales that cannot be observed in operational settings, i.e. 10^2 to 10^4 years.

Aims and hypotheses

This study has three aims: first, to review the work on solubility trapping from previous natural analogue studies. Second, to assess the value of natural analogues as a means of investigating long-term solubility trapping in CCS reservoirs. And third, to test conceptual scenarios of solubility trapping rate over time using results from analogues, engineered reservoirs and models.

In terms of the third aim, there is uncertainty on the relative contribution of dissolution during the injection and post-injection phases of engineered storage. The injection phase is defined as the initial years-to-decades of a CCS project when CO_2 injection is occurring. The post-injection phase refers to the decades of post-injection monitoring followed by the centuries and millennia of long-term storage (>10 kyr). In the post-injection phase, a stable, structurally trapped CO_2 plume would be expected to develop under a caprock in most reservoir settings. Even in well-described reservoirs, the CO_2 dissolution rate and the potential occurrence of equilibrium points are uncertain. The range of outcomes can be summarised by two end-member scenarios for the relative rates of solubility trapping from the start of injection, through to long-term storage (Fig. 1).

Scenario A can be considered the 'rapid decline' dissolution scenario (Fig. 1a). Dissolution rates are initially very high at the start of injection but decline exponentially. In terms of process, this involves rapid mixing of the injected CO_2 plume with formation water by entrapment and displacement. In scenario A an equilibrium point is reached in the post-injection phase. Equilibrium occurs because of the lowered CO_2 fugacity, due to the reduced free-phase volume, and the high CO_2 saturation of the surrounding, hydrostatic formation water. Mineral dissolution and precipitation reactions associated with CO_2 are also in equilibrium. Unless the system is disturbed, the dissolution rate beyond the equilibrium point is zero.

Scenario B can be considered the 'steady decline' dissolution rate scenario (Fig. 1b). Dissolution rates are still highest during injection and occur through the same processes as in scenario A; however, the exponential rate of decay is slower. This is due to diffusion, and potentially convection, persisting throughout the post-injection period. The continued action of these processes over thousands to millions of years results in a delayed equilibrium of the system and a larger mass of CO_2 dissolved.

The occurrence of equilibrium points and the potential persistence of processes like diffusion and convection are influenced by reservoir properties. Different forms of anisotropy and heterogeneity can variably influence dissolution. Uniformly high permeability will enhance plume advancement and enable convection, while the occurrence of low-permeability layers will increase the CO_2-formation water contact area due to CO_2 channelling and capillary effects (Gilmore *et al.* 2020). Different spatial orders of reservoir heterogeneity may variably enhance or inhibit the development of convection (Soltanian *et al.* 2017). Hydrological variables such as the aquifer size and advection will also have effects that are difficult to quantify. The interplay between factors means that, even with quality datasets, a basic prediction of scenario A or scenario B-like behaviour in a CCS reservoir is challenging. Analysis of existing data from the study of natural CO_2 storage analogues and the comparison of numerical and analytical modelling studies can allow the applicability of the end-member scenarios to be tested.

Dissolution in engineered CCS sites

Sleipner, the world's longest running engineered CO_2 storage site, is located in the Norwegian sector of the North Sea. Since injection began in 1996, over 18 million metric tons of CO_2 have been stored to date (Williams & Chadwick 2021). As the longest running engineered CO_2 storage site with a large geophysical monitoring dataset, it provides a decadal timescale estimate of physical and geochemical trapping.

The Miocene-Pliocene age Utsira Formation aquifer at Sleipner has high porosity and permeability of 35% and 2 darcy. The Utsira Formation is approximately 300 m thick and composed of 90% net sandstone, vertically segregated by thin sub-horizontal mudstone beds, which allow for a stacked vertical migration and structural trapping of the CO_2 (Eiken *et al*. 2011; Cavanagh & Haszeldine 2014).

Seabed gravimetry has been the primary means of estimating dissolution rates (Alnes *et al*. 2011) as the absence of reservoir fluid sampling means that other established geochemical techniques cannot be used (Cavanagh 2013). An initial seabed gravimetric survey was acquired in 2002, after 5 million Mt of CO_2 had been injected. Repeat surveys were acquired in 2005, after 8 Mt had been injected, and in 2009, after 11 Mt had been injected. Analysis of the data focussed on determining the density of the CO_2 plume (Nooner *et al*. 2007; Alnes *et al*. 2008). The gravity estimated plume density was compared with the expected CO_2 density from reservoir temperature and pressure conditions, to estimate the proportion of CO_2 dissolved. An upper estimate of the rate of dissolution was 1.8% per year (Alnes *et al.* 2011), equivalent to 13% of the total plume mass in 2009. This rate is broadly similar to the results of independent reactive transport simulation studies which estimated that, by 2011, 10% of the injected CO_2 had dissolved (Chadwick 2013).

We can compare these two published estimates for Sleipner with a simple analytical approximation for the mass of CO_2 dissolved during injection. The initial CO_2 saturation of the formation water at Sleipner was not measured. Here we simplify and assume that the initial formation water is CO_2-free. In an open aquifer setting the dynamically displaced formation water volume, equivalent to 100% of the CO_2 volume, is completely saturated given its direct contact with the advancing CO_2 plume front. An assumed residual formation water pore volume (20% of the plume volume) will also become fully saturated. Using an average CO_2 plume density of 600 kg/m^3 (Cavanagh & Haszeldine 2014), and a dissolved CO_2 density of 50 kg/m^3 for saturated formation water, we estimate that for 11 Mt of injected CO_2, the rapid dissolution response could be as high as 1.15 Mt (229 kt residual + 917 kt displaced), which is approximately 10.5% of the injected mass. The estimate is in broad agreement with the numerical simulation estimate by Chadwick (2013) which also assumes a CO_2-free initial condition for the formation water. The dissolution estimate using geophysical inversion (Alnes *et al.* 2011) is also in agreement. This suggests that, under observed conditions, the formation water appears to be free of dissolved CO_2 prior to injection.

These outcomes indicate significant dissolution at Sleipner during injection. However, the operational timescales of engineered CO_2 storage sites are short. The short timescales necessitate the consideration of natural analogues and models to understand the long-term evolution of CO_2 solubility trapping beyond the injection period.

Dissolution in natural analogues

Noble gas and stable carbon isotope data acquired from producing CO_2 wells at natural analogue reservoirs in the USA, Europe, and China, have been used to establish that CO_2 dissolution is the largest geochemical trapping mechanism over geological timescales, after the primary mechanism of structural and stratigraphic trapping (Gilfillan *et al*. 2009; Zhou *et al*. 2012). The key gas isotopes within the CO_2 for identifying and quantifying dissolution are ^{3}He, ^{4}He, ^{20}Ne, and δ^{13}C.

The ratio of CO_2 to ^{3}He ($CO_2/^3$He) is used to calculate the fraction of CO_2 that has partitioned from the free-phase through either dissolution or mineralisation. These partitions are collectively referred to as free-phase CO_2 removal. CO_2 is soluble in water and reactive with reservoir minerals and dissolved mineral salts. ^{3}He is present in naturally occurring CO_2 at specific concentrations depending on the source of the gas. Significantly, ^{3}He is both inert and insoluble in water (Holland & Gilfillan 2013). Therefore, changes in the free-phase $CO_2/^3$He can be attributed to CO_2 removal at a sampled well location. Using the highest $CO_2/^3$He sample from a given reservoir as the minimum indication of CO_2 removal, a relative removal fraction in each well can be established. This method suggests that for Bravo Dome and McElmo Dome, two large natural analogue fields in the USA, portions of the reservoirs have experienced CO_2 removal of up to 50% at Bravo Dome and up to 90% at McElmo Dome (Gilfillan *et al*. 2009). These are minimum estimates of CO_2 removal, as they are relative to the highest $CO_2/^3$He well sample in the field, which itself may have undergone some degree of CO_2 dissolution or mineralisation.

Dissolution can be identified as the mechanism of CO_2 removal if decreasing $CO_2/^3$He in the gas sample correlates with increased ^{4}He and ^{20}Ne concentrations. ^{4}He and ^{20}Ne originate from different sources but mix in the reservoir formation water. ^{4}He is a by-product of the radioactive decay of U, Th and K atoms found in many minerals. ^{20}Ne is sourced from the atmosphere through dissolution in meteoric water and subsequent percolation into deeper formation waters. In gas samples from several analogue fields, ^{4}He and ^{20}Ne share an inverse relationship with $CO_2/^3$He (Gilfillan *et al*. 2009; Zhou *et al.* 2012). As CO_2 dissolution occurs, $CO_2/^3$He in the gas leg decreases. Independently, the ^{4}He and ^{20}Ne concentrations increase due to their partitioning out of the formation water and into the CO_2. Fig. 2 shows a schematic of the isotope ratio variation that is expected within a reservoir due to the interaction of the CO_2 and water phases.

Dissolution of CO_2 also causes a predictable δ^{13}C fractionation, which is distinct from the fractionation associated with carbonate mineral precipitation. Therefore, the relationship of δ^{13}C to the removal of free-phase CO_2 is used to quantify the percentage removed through dissolution versus mineralisation. A study of nine analogue reservoirs found the largest mineralisation contribution to be within the gas leg of a Bravo Dome well, with up to 18% of CO_2 removal attributed to carbonate precipitation, and the remaining 82% of CO_2 removal attributed to dissolution (Gilfillan *et al*. 2009). The age of CO_2 emplacement in the studied reservoirs is variable, but commonly >1 Ma. Given the geological age, we assume that mineralisation has reached equilibrium but the potential for ongoing mineralisation at slow rates cannot be ruled out.

Different sources of naturally occurring CO_2, such as magmatism, carbonate dissolution and organic processes, produce gas with different δ^{13}C signatures (Wycherley *et al.* 1999). Mixing of CO_2 sources with different $\delta^{13}C$ signatures would complicate the calculation of dissolution and mineralisation. The absolute ^3He concentration and $CO_2/^3He$ of 6 sampled analogue fields in the USA, including Bravo Dome and McElmo Dome, was within the mantle range (Gilfillan *et al.* 2008; Gilfillan *et al.* 2009). The minor occurrence of carbonate or organic derived CO_2 cannot be ruled out but would be a minor contributor relative to the primary magmatic source. Therefore, a single uniform magmatic source was assumed in all calculations.

Analogue studies

Bravo Dome is an exceptionally large CO_2 field, containing more than one billion metric tonnes (Gt) of CO_2, which has been in production since 1981. A large gas isotope dataset has been acquired by sampling producing wells. Geochemistry has helped to establish conceptual models of emplacement and original CO_2 mass. The models also estimate the fraction of CO_2 lost to dissolution and, to a first approximation, average long-term dissolution rates. However, the two recently published models of dissolution rates at the field differ because of significantly different age estimates for the CO_2 emplacement event (Sathaye *et al*. 2014; Zwahlen *et al*. 2017).

To the authors' knowledge, Bravo Dome is the only natural analogue where quantitative estimates of dissolved CO_2 mass have been performed. These field studies demonstrate a methodology that could be applied to other analogue reservoirs where gas sampling is possible. Reservoirs where the age of CO_2 arrival is corroborated by multiple independent tests would give more clarity on long-term rates of dissolution.

Bravo Dome has several features that are atypical of reservoirs considered for CO_2 storage. The gigatonne scale of Bravo Dome is one-to-two orders of magnitude larger than most planned sites. Additionally, the reservoir is highly heterogeneous, under-pressured, and shallow at 700 m below surface (Sathaye *et al.* 2016). The latter two conditions result in a low-density gas phase, whereas engineered sites prefer a denser, super-critical, phase to improve storage capacity. Additionally, a significant area of the reservoir sits directly above an impermeable granitic basement with no gas-water contact (GWC) (Zwahlen *et al.* 2017). The differences hamper a direct comparison with Sleipner, an exemplar of a deep saline aquifer setting (Arts *et al*. 2004).

Reservoir thickness, porosity, and pre-production pressure mapping provided an estimate of CO_2 mass per unit area. The free-phase CO_2 mass prior to production was estimated to be 1.3 ± 0.6 Gt (Sathaye *et al*. 2014). Mapping $CO_2/^3He$ across the field led to estimated free-phase CO_2 removal of 366 ± 120 Mt. As mineralisation was shown to be a secondary contributor to free-phase CO_2 removal (Gilfillan *et al*. 2009), the calculations were simplified to attribute all removal to dissolution. By ignoring the removal of CO_2 by mineralisation the results overestimated dissolution at individual sample points by up to 18%. By combining pre-production mass with the calculated dissolved mass, the original emplaced CO_2 mass was estimated to be 1.6 ± 0.67 Gt (Sathaye *et al*. 2014). The error margins for both the original emplaced CO_2 mass and the mass removed through dissolution are large and are primarily caused by variance in reservoir depth (Sathaye *et al.* 2014). The error margins lead to a CO_2 dissolution estimate of 11–52%.

The calculated mass of dissolved CO_2 can be converted into an average dissolution rate using estimates of emplacement timing. Sathaye *et al*. (2014), assumed that the magmatic CO_2 was sufficiently hot to exceed an apatite closure temperature of 75°C at the reservoir entry point. Age dates of apatite minerals from reservoir core samples were used to constrain the timing of CO_2 emplacement. The method produced an age of 1.2–1.5 Ma, falling within the broad range of 56 ka–1.7 Ma established by dating local igneous rocks proposed to be the source of the magmatic CO_2 (Nereson *et al*. 2013).

Sathaye *et al*. (2014) assumed that 40% of the total dissolution occurred in the first 5 kyr after emplacement, followed by much slower dissolution over the remainder of the residence time. This is similar to our scenario B. The initial phase of relatively fast dissolution is attributed to high capillary entry pressures in siltstones: during emplacement, Sathaye *et al*. (2014) assumed that CO_2 would have displaced the formation water in the reservoir sandstones but not the siltstones, leaving a large volume of unsaturated formation water above the GWC. The CO_2 could saturate the formation water in the siltstones through diffusion. Based on log data, the average thickness of siltstone layers is less than 10 m. Sathaye *et al.* (2014) predicted that diffusive transport would fully saturate the siltstones within 5 kyr. The slower, longer-term dissolution was attributed to diffusion across the stabilised GWC. In one sector of the field, the authors estimated a dissolution flux greater than that expected for diffusion and inferred localised density-driven convection to explain the discrepancy.

Zwahlen *et al.* (2017) took a different approach, firstly using a higher ^{3}He baseline sample of 7.4 x 10^9 compared to 5.35×10^9 in Sathaye *et al.* (2014). This results in a larger total emplaced CO_2 mass of 1.8 ± 0.67 Gt and larger free-phase CO_2 removal of 506 ± 166 Mt. The error limits are borrowed from the Sathaye *et al.* (2014) study, and so remain large. Using the endpoints produced an estimate for CO_2 dissolution of 14–59%.

Zwahlen *et al.* (2017) estimated a CO_2 emplacement age of 14–17 ka, based on noble gas and stable isotope diffusion profiles from the GWC through the gas column. This is much younger than the 1.2–1.5 Ma estimated by Sathaye *et al*. (2014) and approximately 40 kyr younger than the earliest age date for local igneous rocks (Nereson *et al*. 2013).

The far younger emplacement age and larger estimate of dissolved CO_2 in Zwahlen *et al*. (2017) produces an average dissolution rate approximately 100 times greater than Sathaye *et al.* (2014) (Table 1). An explanatory dissolution model was not proposed. However, the dissolution of around 500 Mt of CO_2 in under 20 kyr would require a rapid model, potentially with a significant convection component, as the diffusive flux rates inferred by Sathaye *et al.* (2014) are insufficient to account for the estimated dissolution over a much longer timescale.

Data from Jackson Dome, Mississippi, another large natural CO_2 reservoir in the USA, supports an exponential decrease in dissolution rate over time, with the majority of CO_2 dissolution occurring during the initial migration and emplacement phase. Like the studies from Bravo Dome, measurements of $CO_2/^3He$ were used to determine free-phase CO_2 removal, and $\delta^{13}C$ data were used to quantify the role of dissolution versus mineralisation. Greater proportions of dissolution and increased CO_2-water interaction, indicated by ^{4}He and ^{20}Ne, were observed at the field crest compared to the flanks (Zhou *et al*. 2012). The variation in dissolution from crest to flanks supports a model of rapid decline in dissolution rate. Due to buoyancy, CO_2 reservoirs fill from the top down. CO_2 trapped at the crest will have been at the front of the plume and will have displaced the ambient formation water during migration. High rates of dissolution will have occurred when the CO_2 contacted this formation water. Later CO_2 charge, which filled the flanks of the reservoir will have had less contact with under-saturated formation water during migration. CO_2 at the flank, will be in closer proximity to the GWC, which is established when the plume has stabilised. Despite being closer to the hydrostatic formation water during storage, the flank samples record less CO_2 dissolution than the crest. This suggests that diffusion or convection related dissolution, after plume stabilisation, is less significant than dissolution during the initial emplacement and migration.

Modelled dissolution rates

Analytical models and numerical simulations have been used to gain an understanding of the controls and rates of CO_2 dissolution. These models can be compared with estimates from natural analogues and engineered sites. We have compiled data from eight modelling studies (Table 2) that report dissolved CO_2 over time (Ozah *et al*. 2005; Pickup *et al*. 2011; Pruess & Nordbotten 2011; Sato *et al*. 2011; Bonneville *et al*. 2013; Szulczewski *et al*. 2013; Kempka *et al*. 2014; Orsini *et al*. 2014). All studies are reservoir-scale simulations. The smallest 2D simulation included in the analysis has a length of 5 km and a thickness 200 m (Szulczewski *et al*. 2013) and the smallest 3D simulation has a volume of 1×10^9 m^3 (Sato *et al*. 2011). All models used realistic generic reservoir properties or were based on specific prospective or operational storage sites. In some studies, multiple scenarios with different reservoir properties or model boundary conditions were simulated. In these cases, scenarios described as a 'reference' or 'base case' were used. In studies without a clear reference case, the scenario which produced the median case result, in terms of total cumulative dissolution, was selected. Further details on the selected studies are provided in the supplementary information.

Using the model studies, we have calculated the fraction of injected CO_2 that has dissolved and the average dissolution rates, i.e., the total mass of CO_2 dissolved over the duration of CO_2 residence time. The dissolution fraction and average dissolution rates allow for a comparison of the conformance of the Bravo Dome and Sleipner estimates with modelling results. In Fig. 3, the fraction of CO_2 that has dissolved is plotted against the storage duration time.

Dissolution can be normalised to the total mass of CO_2 injected or emplaced to allow for a comparison of dissolution between scenarios at different scales (Figs. 4 and 5). In Fig. 4, the area of the circles represents the total mass of CO_2 injected or emplaced in each study. The normalisation resolves the average fraction of dissolved CO_2 per year relative to the total CO_2 mass. We use the fraction of total CO_2 dissolved per year as a metric for dissolution instead of dissolution per GWC area. Dissolution per GWC area does not correctly scale results during the migration phase, because a stable GWC has not developed, and is further complicated by the variety of different GWC geometries in different reservoirs. For example, in Bravo Dome only half of the reservoir is in contact with the aquifer, while in Sleipner multiple stacked contacts within the aquifer are present.

Of the eight selected model studies, six reported the change in cumulative dissolved CO_2 over time. These plots of cumulative dissolved CO_2 were digitised (Rohatgi, 2020) and converted to plots of dissolution rate over time. These dissolution rate data are normalised to the fraction of total CO_2 dissolved per year and summarised by exponential or power law functions to best fit each study (Fig. 6). The time averaged dissolution rates from natural and engineered CO_2 reservoirs are also plotted for comparison.

Modelled study results

The model studies included in the analysis show a weak trend of increasing CO_2 dissolution with longer simulation duration (Fig. 3). The weakness of the correlation reflects the significant variation in many of the variables that influence dissolution (e.g. boundary conditions, reservoir porosity and permeability, heterogeneity, fluid pressure and temperature). The Alnes *et al.* (2011) Sleipner dissolution fraction, after 13 years of storage, fits the middle trend for the model studies. The mid-case dissolved fractions from the 'young' Bravo Dome estimate of 15.5 ka (Zwahlen *et al.* 2017) and the 'old' estimate of 13.5 Ma (Sathaye *et al.* 2014) plot below the trend. However, the large error bars in the Bravo Dome studies mean they could potentially fit a wide range of trends. The two opposing models for Bravo Dome share a similar range for fraction of CO_2 dissolved, despite the greatly differing age estimates. Regardless of which Bravo Dome age estimate is assumed to be correct, the results show that when corrected for scale, total dissolution in Bravo Dome is relatively low when compared to most equivalent model studies. Even when taking the maximum values from their respective error ranges, the Bravo Dome studies plot significantly below a group of models predicting higher fractions of CO_2 dissolved over shorter timescales. Normalising to total CO_2 mass does not fully correct for the decrease in surface area per unit mass of CO_2 in larger scale studies. The lower dissolution percentage in the Bravo Dome studies are partly due to lower CO_2 surface area- to-CO_2 mass ratios.

Fig. 4 shows scaled average dissolution rates over the storage and simulation duration with circle areas equivalent to the total mass of CO_2 injected or emplaced. On the log-log plot there is an approximate linear trend of reducing dissolution rate with increased storage duration. This trend is expected, as the variables are related. A relationship of longer storage duration studies considering larger CO_2 masses is also observed. The contrast in circle area illustrates the scale dichotomy of Bravo Dome relative to Sleipner and most of the model studies. Excluding the analytical study by Szulczewski *et al*. (2013), the CO_2 masses in Bravo Dome are at least one order of magnitude larger than numerical model studies. A study where 100% of the CO_2 has dissolved (Szulczewski *et al.* 2013) plots directly on the upper trend line. Long duration studies whose midpoints plot significantly below the upper line, such as the two Bravo Dome studies (Sathaye *et al*. 2014; Zwahlen *et al.* 2017), are interpreted to represent equilibrium being reached with a relatively small fraction of CO_2 dissolved. Shorter duration studies that show low fractions of dissolution, like the Sleipner gravity study (Alnes *et. al*. 2011), can be partly explained by the short operational timescales. The injected CO_2 is likely not in equilibrium with the formation water and dissolution is currently ongoing.

Fig. 5 shows the central cluster of points from Fig. 4 plotted linearly up to 20 kyr. On a scale of linear time, we observe a non-linear decline in the fraction of CO_2 dissolved per year with increased storage time. The rate of decline supports a model of rapid initial rates of dissolution, followed by negligible rates over geological timescales. The common trend of the model studies and the analogue estimate shows that the models and analogues share similar average dissolution rate versus storage duration behaviour.

If a model of rapid dissolution rate decline is favoured, and a steady decline dissolution model rejected, then calculated dissolution rates from the Bravo Dome analogues can be reconsidered assuming a significant time-period of equilibrium prior to the samples being collected. The Bravo Dome studies (Sathaye *et al*. 2014; Zwahlen *et al*. 2017) show similar mid-case estimates of the fraction of CO_2 dissolved despite the greatly different age estimates. The insensitivity of the fraction of CO_2 dissolved to the storage duration suggests a significant period of storage time after equilibrium has been reached in Bravo Dome. Additional time after 14–17 kyr storage duration does not increase the cumulative dissolved CO_2 and therefore dissolution rates beyond such timescales may be negligible.

The potential of dissolution rate reaching equilibrium (i.e. zero dissolution) reframes the apparent dissolution rate by requiring the inclusion of a stasis period in the calculation. A rapid decline model for Sleipner (Fig. 1a), would imply that approximately 40% of dissolution occurs during injection (around 10% of the total injected CO_2), and that dissolution is complete within a few hundred years (25% of the stored mass), with 80% of the dissolution occurring within 100 years. The alternative, a steady decline model (Fig. 1b), would initially result in a similar amount of injection related dissolution (10% of total injected CO_2). A much longer tail to dissolution of around 1000 years results in approximately 50% of the injected CO_2 dissolving, with 80% of the dissolution occurring after 300 years.

The scaled dissolution rate over time plots (Fig. 6) show a simplified evolution of the model study dissolution rates, with a rapid decline over time. The analogue histories are too uncertain to constrain the onset of stasis, indicating a need for modelling and analogue studies to be combined when predicting the long-term rate of solubility trapping in CCS storage sites.

Discussion

The geological CO_2 storage timescales that natural analogues represent will be of interest to many stakeholders. However, it is important to recognise the limitations of analogue studies. The mapping and quantification of subsurface reservoirs is an interpretative and uncertain process due to the relative scarcity of data. Even in ideal settings, the extrapolation of geochemical data between wells entails uncertainty in the estimates of initial CO_2 mass and the fraction dissolved. Bravo Dome is presently the most studied analogue with respect to CO_2 dissolution, but the size, depth, pressure, and gas-water contact configuration are atypical of CCS sites (Sathaye *et al*. 2016). Our synthesis of data suggests that the large size of the reservoir can be partly corrected for, but future studies should focus on analogue sites that more closely represent expected reservoir conditions for CCS sites. This will increase the relevance of analogue results by minimising the influence of atypical factors.

Greatly differing age estimates have been proposed for Bravo Dome. Sathaye *et al.* (2014) estimate an age of 1.2–1.5 Ma, compared to 14–17 ka proposed by Zwahlen *et al.* (2017). The age uncertainty illustrates a need for analogue sites with well-constrained emplacement timings. At Bravo Dome, there is also a large uncertainty associated with the original emplaced CO_2 mass and dissolved mass, which originates from uncertainty in the reservoir depth and thickness used in the volume calculation. The potentially large errors caused by subsurface uncertainty highlights a need for selecting analogues sites with improved well control and supporting seismic data where available. The simplifying assumption adopted by Sathaye *et al*. (2014) and Zwahlen *et al*. (2017), attributing all removal to dissolution, also introduces an error that can be reduced by considering the CO_2 lost through mineralisation. Ideally, analogue studies require a holistic physical-chemical model for dissolution and mineralisation that can explain the calculated masses and rates. New studies on additional natural CO_2 reservoirs would help to better resolve dissolution rates over geological timescales and improve models of CO_2 trapping and storage security in engineered reservoirs.

At Jackson Dome, CO_2 dissolution is greatest at the reservoir crest and lowest at the flanks (Zhou *et al*. 2012). The greater dissolution at the crest suggests that most dissolution occurs during migration and emplacement before the establishment of a stable gas-water contact (GWC). We interpret that the high rates of dissolution during migration and emplacement are because of the mobile plume displacing and mixing with a large volume of formation water that is not fully saturated in CO_2. The significance of GWC proximity and surface-area on dissolution implied by this observation needs to be investigated in more analogue reservoirs. If GWC proximity and surface-area correlate with increased dissolution, this would support a model for sustained, post-emplacement dissolution across the GWC. An inverse correlation would support a model of rapid and early dissolution during the migration and emplacement phase. The occurrence of significant dissolution during migration and emplacement has implications for dissolution rate quantification. A metric in current use is CO_2 flux, i.e. dissolved CO_2 mass per GWC contact area per year ($g/m^2/yr$). This metric would be of limited use if most of the dissolution occurs prior to the establishment of a stable gas-water contact.

Further work on the conceptual model is expected to formalise a two-stage approach that will examine the initial dynamic phase of injection and emplacement and the much longer stabilising phase that follows prior to equilibrium. The significance, and ubiquity of the density-driven convection of CO_2 saturated formation water is not yet established in either phase. The current conceptual model discussed is simple and applies across different reservoirs and injection scenarios. The evolution of dissolution rate over geological time in natural analogues remains highly uncertain and may include a long but elusive stasis phase in hydrostatic settings. Hydrodynamic settings, where a strong aquifer drive is present, will likely require a separate approach. We propose that more research should focus on further quantification of dissolution mass and rate in naturally occurring CO_2 reservoirs that reflect expected regional conditions for areas such as the North Sea, Gulf of Mexico and continental North America.

The comparison of CO_2 dissolution between analogues, engineered reservoirs and model studies shows a range of behaviour. The results from Sleipner and Bravo Dome do not align with a trend of 60–80% solubility trapping within a few thousand years, which some models predict. A potential contributing factor to the lower dissolution in analogue and engineered reservoirs could be small-scale geological heterogeneity influencing diffusion and convection in ways not captured in numerical and analytical simulations. Additionally, the numerical and analytical simulations assume formation water that is initially free from dissolved CO_2. In cases where the initial saturation is unknown and models assume CO_2-free formation water as an initial condition, the results should be interpreted as an upper limit to CO_2 dissolution.

Our results are relevant to CCS decision makers. Demonstration of significant dissolution of injected CO_2 during a project's operational lifetime would contribute a material increase in the reservoir storage capacity. For example, if approximately 10% of a plume dissolves during injection due to saturation of the displaced plume volume and residual formation water trapped within the plume, this may reduce the required reserves for European CO_2 storage by as much as a gigatonne before 2050. Recognition of solubility trapping as an important process could also encourage operators to acquire data on the baseline CO_2 saturation of the reservoir prior to injection. An assayed baseline would allow for a more accurate prediction of solubility trapping. Acquisition of repeat samples, after the start of injection, would allow a confident quantification of solubility trapping on operational timescales.

Conclusion

Trapping is the essential component of secure CO_2 storage, and solubility trapping makes a significant contribution to the removal of free-phase CO_2 in both natural and engineered reservoirs. Dissolution is likely to remove at least 10% and as much as 50% of the total free-phase CO_2 mass over the lifetime of a storage site.

Natural CO_2 reservoirs provide insights on the long-term fate of CO_2 in storage reservoirs. $CO_2/^3He$, ^4He, ^{20}Ne and $\delta^{13}C$ data from natural CO_2 reservoirs can produce estimates of the CO_2 mass dissolved and the dissolution rate. These data show that solubility trapping removes a significant fraction of free-phase CO_2, thereby enhancing storage security. Quantitative estimates of CO_2 dissolution from Bravo Dome, USA show solubility trapping has removed at least 300 Mt of CO_2 over a minimum of 10 kyr.

Evidence from another North American analogue site, Jackson Dome, supports a model of most dissolution occurring during initial migration and emplacement. Indications from gravimetric data at Sleipner show solubility trapping of around 10% of CO_2, during the operational lifetime of a storage site, i.e. decades. The significance of dissolution of during the initial stages of CO_2 storage means that much of the process is observable during the site's operational period, whereas metrics quantifying CO_2 dissolution by contact area with a stable GWC are less effective, as the stable contact is a post-emplacement feature.

Analytical and numerical model studies predict a wide range of percentage dissolution. In some cases, dissolution in excess of 60–80% of injected CO_2 is predicted. Such high percentages of dissolution have not been observed on a reservoir-scale at Bravo Dome. Additional studies of natural analogue reservoirs are required to better understand the credible range of dissolved CO_2 mass and CO_2 dissolution rate in CCS reservoirs on millennial timescales.

Acknowledgements

RL is funded by NERC through an E4 DTP studentship NE/S007407/1, and Equinor ASA, with no influence on the results. AJC and RSH are funded by UKCCSRC2017 EPSRC EP/P026214/1, and RSH by SCCS (Scottish Funding Council) and HyStorPor EPSRC EP/S027815/1. GJ is funded by the University of Strathclyde Faculty of Engineering. SMVG is funded by NERC grant NE/R018049/1, EPSRC grants EP/P026214/1 and EP/K036033/1 and Total E & P, with no influence on results.

Author Roles

RL wrote most of the article, co-created the figures and carried out the analysis of the data. AJC made significant contributions to the manuscript, conceptual model and co-created the figures. RSH critiqued the manuscript and developed the structure of the paper. GJ critiqued the manuscript and made contributions to the introduction and dissolution in natural analogues sections. SMVG developed the initial concepts, made significant contributions to the manuscript and secured funding for the study.

Data access statement

All data generated or analysed during this study are included in this published article and its supplementary information files.

References

Ajayi, T., Gomes, J. S. and Bera, A. 2019. A review of CO_2 storage in geological formations emphasizing
modeling, monitoring and capacity estimation approaches. *Petroleum Science,* **16**, 1028-1063, https://doi.org/10.1007/s12182-019-0340-8

Alcalde, J., Flude, S., Wilkinson, M., Johnson, G., Edlmann, K., Bond, C. E., Scott, V. Gilfillan, S. M. V., Ogaya, X. and Haszeldine, R. S. 2018. Estimating geological CO_2 storage security to deliver on climate mitigation. *Nature Communications*, **9**, 2201, https://doi.org/10.1038/s41467-018-04423-1

Allis, R., Chidgey T., Gwynn, W., Morgan, C., White, S., Adams, M. and Moore, J. 2001. Natural CO_2 reservoirs on the Colorado Plateau and southern Rocky Mountains: Candidates for CO_2 sequestration. *In*: Proceedings of the First National Conference on Carbon Sequestration, 14-17 May 2001, Washington DC, USA.

Alnes, H., Eiken, O. and Stenvold, T. 2008. Monitoring gas production and CO_2 injection at the Sleipner field using time-lapse gravimetry. *Geophysics*, **73**, WA155-WA161, https://doi.org/10.1190/1.2991119

Alnes, H., Eiken, O., Nooner. S., Sasagawac, G., Stenvold, T and Zumberge M. 2011. Results from Sleipner gravity monitoring: Updated density and temperature distribution of the CO_2 plume. *In*: Gale, J., Hendriks, C. and Turkenberg, W. (eds) *Energy Procedia*. 10th International Conference on

Greenhouse Gas Control Technologies, 19-23 September 2010, Amsterdam, The Netherlands, **4**, 5504-5511, https://doi.org/10.1016/j.egypro.2011.02.536

Arts, R., Eiken, O., Chadwick, A., Zweigel, P., van der Meer, L. and Zinszner, B. 2004. Monitoring of CO_2 injected at Sleipner using time-lapse seismic data. *Energy*, **29**, 1383-1392, https://doi.org/10.1016/j.energy.2004.03.072

Bonneville, A., Gilmore, T., Sullivan, C., Vermeul, V., Kelley, M., White, S., Appriou, D., Bjornstad, B., *et al*. 2013. Evaluating the Suitability for CO_2 Storage at the FutureGen 2.0 Site, Morgan County, Illinois, USA. *In*: Dixon, T. and Yamaji, K. (eds) *Energy Procedia*. Proceedings of the 11th International Conference on Greenhouse Gas Control Technologies, 18-22 November 2012, Kyoto, Japan, **37**, 6125-6132, https://doi.org/10.1016/j.egypro.2013.06.541

Cavanagh, A. 2013. Benchmark Calibration and Prediction of the Sleipner CO_2 Plume from 2006 to 2012. *In*: Dixon, T. and Yamaji, K. (eds) *Energy Procedia*. Proceedings of the 11th International Conference on Greenhouse Gas Control Technologies, 18-22 November 2012, Kyoto, Japan, **37**, 3529-3545, https://doi.org/10.1016/j.egypro.2013.06.246

Cavanagh, A. J. and Haszeldine, R. S. 2014. The Sleipner storage site: Capillary flow modeling of a layered CO_2 plume requires fractured shale barriers within the Utsira Formation. *International Journal of Greenhouse Gas Control*, **21**, 101-112, https://doi.org/10.1016/j.ijggc.2013.11.017

Chadwick, R. A. 2013. Offshore CO_2 storage: Sleipner natural gas field beneath the North Sea. *In*: Gluyas, J. and Mathias, S. (eds.) *Geological Storage of Carbon Dioxide (CO_2)*. Woodhead, 227-250, https://doi.org/10.1533/9780857097279.3.227

Eiken, O., Ringrose, P., Hermanrud, C., Nazarian, B., Torp, T. and Høier, L. 2011. Lessons learned from 14 years of CCS operations: Sleipner, In Salah and Snøhvit. *In*: Gale, J., Hendriks, C. and Turkenberg, W. (eds) *Energy Procedia*. 10th International Conference on Greenhouse Gas Control Technologies, 19-23 September 2010, Amsterdam, The Netherlands, **4**, 5541-5548, https://doi.org/10.1016/j.egypro.2011.02.541

Gilfillan, S. M. V., Ballentine, C. J., Holland, G., Blagburn, D., Sherwood Lollar, B., Stevens, S., Schoell, M. and Cassidy, M. 2008. The noble gas geochemistry of natural CO_2 gas reservoirs from the Colorado Plateau and Rocky Mountain provinces, USA. *Geochimica et Cosmochimica Acta*, **72**, 1174-1198, https://doi.org/10.1016/j.gca.2007.10.009

Gilfillan, S. M. V., Sherwood Lollar, B., Holland, G., Blagburn, D., Stevens, S., Schoell, M., Cassidy, M., Ding, Z., Zhou, Z., Lacrampe-Couloume, G. and Ballentine, C. J. 2009. Solubility trapping in formation water as dominant CO2 sink in natural gas fields. *Nature*, **458**, 614-618, https://doi.org/10.1038/nature07852

Gilmore, K. A., Neufeld, J. A. and Bickle, M. J. 2020. CO_2 Dissolution Trapping Rates in Heterogenous Porous Media. *Geophysical Research Letters*, **47**, e2020GL087001, https://doi.org/10.1029/2020GL087001

Haszeldine, R. S., Quinn, O., England, G., Wilkinson, M., Shipton, Z. K., Evans, J. P., Heath, J., Crossey, L., Ballentine, C. J. and Graham, C. M. 2005. Natural Geochemical Analogues for Carbon Dioxide Storage in Deep Geological Porous Reservoirs, a United Kingdom Perspective. *Oil & Gas Science and Technology*, **60**, 33–49, https://doi.org/10.2516/ogst:2005004

Holland, G. and Gilfillan, S. 2013. Application of Noble Gases to the Viability of CO_2 Storage. *In*: Burnard P. (ed.) *The Noble Gases as Geochemical Tracers. Advances in Isotope Geochemistry*. Springer, 177-223, https://doi.org/10.1007/978-3-642-28836-4_8

Jacob, R. and Saylor, B. Z. 2016. CO_2 solubility in multi-component brines containing NaCl, KCl, CaCl2 and MgCl2 at 297 K and 1-14 MPa. *Chemical Geology*, **424**, 86-95, https://doi.org/10.1016/j.chemgeo.2016.01.013

Kempka, T., De Lucia, M. and Kühn, M. 2014. Geomechanical integrity verification and mineral trapping quantification for the Ketzin CO_2 storage pilot site by coupled numerical simulations. *In*: Dixon, T., Herzog, H. and Twinning, S. (eds) *Energy Procedia*. 12th International Conference on Greenhouse Gas Control Technologies, 5-9 October 2014, Austin, USA, **63**, 3330-3338, https://doi.org/10.1016/j.egypro.2014.11.361

Martinez, M. J. and Hesse M. A. 2016. Two-phase convective CO_2 dissolution in saline aquifers. *Water Resources Research*, **52**, 585-599, https://doi.org/10.1002/2015WR017085

Majer, V., Sedlbauer, J. and Bergin, G. 2008. Henry's law constant and related coefficients for aqueous hydrocarbons, CO_2 and H_2S over a wide range of temperature and pressure. *Fluid Phase Equilibria*, **272**, 65-74, https://doi.org/10.1016/j.fluid.2008.07.013

Miocic, J. M., Gilfillan, S. M. V., Roberts, J. J., Edlmann, K., McDermott, C. I. and Haszeldine R. S. Controls on CO_2 storage security in natural reservoirs and implications for CO_2 storage site selection. *International Journal of Greenhouse Gas Control*, **51**, 118-125, https://doi.org/10.1016/j.ijggc.2016.05.019

Nereson, A., Stroud, J., Karlstrom, K., Heizler, M. and McIntosh, W. 2013. Dynamic topography of the western Great Plains: Geomorphic and 40Ar/39Ar evidence for mantle-driven uplift associated with the Jemez lineament of NE New Mexico and SE Colorado. *Geosphere*, **9**, 521-545, https://doi.org/10.1130/GES00837.1

Newmark, R. L., Friedmann, S. J. and Carrol, S. A. 2010. Water Challenges for Geologic Carbon Capture
and Sequestration. *Environmental Management*, **46**, 651-661, https://doi.org/10.1007/s00267-010-9434-1

Nooner, S. L., Eiken, O., Hermanrud, C., Sasagawa, G. S., Stenvold, T. and Zumberge, M. A. 2007. Constraints on the *in situ* density of CO_2 within the Utsira formation from time-lapse seafloor gravity measurements. *International Journal of Greenhouse Gas Control*, **1**, 198-214, https://doi.org/10.1016/S1750-5836(07)00018-7

Orsini, P., Cantucci, B. and Quattrocchi, F. 2014. Large-scale Numerical Modelling of CO_2 Injection and Containment Phases for an Italian Near-coast Reservoir Using PFLOTRAN. *In*: Røkke, N, A. and Svendsen, H. (eds) *Energy Procedia*. 7th Trondheim Conference on CO_2 capture, Transport and Storage, 4-6 June 2013, Trondheim, Norway, **51**, 334-343, https://doi.org/10.1016/j.egypro.2014.07.040

Ozah, R. C., Lakshminarasimhan, S., Pope, G. A., Sepehrnoori, K., and Bryant, S. L. 2005. Numerical Simulation of the Storage of Pure CO_2 and CO_2-H2S Gas Mixtures in Deep Saline Aquifers. Paper SPE 97255, presented at the SPE Annual Technical Conference and Exhibition, 9-12 October 2005, Dallas, USA, https://doi.org/10.2118/97255-MS

Pickup, G. E., Jin, M., Olden, P., Mackay, E. J. and Sohrabi, M. 2011. A Sensitivity Study on CO_2 Storage in Saline Aquifers. Paper SPE 143054, presented at the SPE EUROPEC/EAGE Annual Conference and Exhibition, 23-26 May 2011, Vienna, Austria, https://doi.org/10.2118/143054-MS

Pruess, K. and Nordbotten, J. 2011. Numerical Simulation Studies of the Long-term Evolution of a CO_2 Plume in a Saline Aquifer with a Sloping Caprock. *Transport in Porous Media*, **90**, 135-151, https://doi.org/10.1007/s11242-011-9729-6

Pruess, K. and Spycher, N. 2007. ECO2N - A fluid property module for the TOUGH2 code for studies of CO_2 storage in saline aquifers. Energy Conversion and Management, **48**, 1761-1767, https://doi.org/10.1016/j.enconman.2007.01.016

Riaz, A. and Cinar, Y. 2014. Carbon dioxide sequestration in saline formations: Part I-Review of the modeling of solubility trapping. *Journal of Petroleum Science and Engineering*, **124**, 367-380, https://doi.org/10.1016/j.petrol.2014.07.024Rohatgi, A. 2020. WebPlotDigitizer version 4.3, https://automeris.io/WebPlotDigitizer

Sathaye, K. J., Hesse, M. A., Cassidy, M. and Stockli, D. F. 2014. Constraints on the magnitude and rate of CO_2 dissolution at Bravo Dome natural gas field. *Proceedings of the National Academy of Sciences of the United States of America*, **43**, 15332-15337, https://doi.org/10.1073/pnas.1406076111

Sathaye, K. J., Smye, A. J., Jordan, J. S. and Hesse, M. A. 2016. Noble gases preserve history of retentive continental crust in the Bravo Dome natural CO_2 field, New Mexico. *Earth and Planetary Science Letters*, **443**, 32-40, https://doi.org/10.1016/j.epsl.2016.03.014

Sato, K., Mito, S., Horie, T., Ohkuma, H., Saito, H., Watanabe, J. and Yoshimura, T. 2011. Monitoring and simulation studies for assessing macro- and meso-scale migration of CO_2 sequestered in an onshore aquifer: Experiences from the Nagaoka pilot site, Japan. *International Journal of Greenhouse Gas Control*, **5**, 125-137, https://doi.org/10.1016/j.ijggc.2010.03.003

Soltanian M. R., Amooie, M. A., Gershenzon, N., Dai, Z., Ritzi, R., Xiong, F., Cole, D. and Moortgat, J. 2017. Dissolution Trapping of Carbon Dioxide in Heterogeneous Aquifers, *Environmental Science & Technology*, **51**, 7732-7741, https://doi.org/10.1021/acs.est.7b01540

Spycher, N. and Pruess, K. 2005. CO_2-H_2O mixtures in the geological sequestration of CO2. II. Partitioning in chloride brines at 12-100°C and up to 600 bar. *Geochimica et Cosmochimica Acta*, **69**, 3309-3320, https://doi.org/10.1016/j.gca.2005.01.015

Steel, L., Liu, K., Mackay, E. and Maroto-Valer, M. M. 2016. CO_2 solubility measurements in brine under reservoir conditions: A comparison of experimental and geochemical modeling methods. *Greenhouse Gas Science and Technology*, **6**, 197-217, https://doi.org 10.1002/ghg.1590

Szulczewski, M. L., Hesse, M. A. and Juanes, R. 2013. Carbon dioxide dissolution in structural and stratigraphic traps. *Journal of Fluid Mechanics*, **736**, 287-315, https://doi.org/10.1017/jfm.2013.511

Williams, G. A. and Chadwick, R. A. 2021. Influence of reservoir-scale heterogeneities on the growth, evolution and migration of a CO_2 plume at the Sleipner Field, Norwegian North Sea. *International Journal of Greenhouse Gas Control*, **106**, 103260, https://doi.org/10.1016/j.ijggc.2021.103260

Wycherley, H., Fleet, A. and Shaw, H. 1999. Some observations on the origins of large volumes of carbon dioxide accumulations in sedimentary basins. *Marine and Petroleum Geology*, **16**, 489-494, https://doi.org/10.1016/S0264-8172(99)00047-1

Zhou, Z., Ballentine, C. J., Schoell, M. and Stevens, S. H. 2012. Identifying and quantifying natural CO_2 sequestration processes over geological timescales: The Jackson Dome CO_2 Deposit, USA. *Geochimica et Cosmochimica Act*, **86**, 257-275, https://doi.org/10.1016/j.gca.2012.02.028

Zwahlen, C, A., Kampman, N., Dennis, P., Zhou, Z. and Holland, G. 2017. Estimating carbon dioxide residence time scales through noble gas and stable isotope diffusion profiles. *Geology*, **45**, 995-998, https://doi.org/10.1130/G39291.1

Figure captions

Fig. 1: Alternative scenarios for the evolution of CO_2 dissolution rate (orange) and cumulative CO_2 dissolution (blue) in storage reservoirs: (**a**) Dissolution rates are high during the injection phase and decline rapidly; dissolution rates are low in the post-injection phase and decline to zero when equilibrium is reached. (**b**) Dissolution rates are high during the injection phase but decline less rapidly and continue after stabilisation of the CO_2 plume. This requires the occurrence of significant dissolution across the gas-water contact by diffusion and potentially convection. The expected injection duration is decades. The storage duration would extend to 10^4 to 10^6 years depending on the specific case study and underlying assumptions.

Fig. 2: Schematic of CO_2-water interactions during dissolution. (**a**) The reservoir is charged with CO_2 and trace gases including ^3He. The formation water contains ^4He and ^{20}Ne that are not present in the CO_2. (**b**) CO_2 dissolves into the formation water and ^4He and ^{20}Ne partition into the CO_2 at varying rates across the reservoir. (**c**) Gas sampled from wells establishes the relative CO_2 removal. ^4He and ^{20}Ne establish the formation water-CO_2 interactions. In this example, lower rates of dissolution in well 1 are evidenced by higher $CO_2/^3He$ and lower ^4He and ^{20}Ne concentrations relative to well 2.

Fig. 3: Fraction of total CO_2 dissolved over duration of simulation or residence time. The data groups into three trends: (a) high rates and high impacts, resulting in 60% to 80% dissolution within a few thousand years; (b) moderate rates and impacts, resulting in 30% to 40% dissolution within tens of thousands of years; and (c) low rates and impacts, resulting in less than 20% dissolved within a hundred thousand years. Best-fit lines, dashed, are approximate and plot as exponential decay curves in non-log space. Bravo Dome studies and Kempka *et al.* (2014) model include min-max ranges. Sleipner gravity inversion (Alnes *et al.* 2011); Bravo Dome geochemistry (Sathaye *et al.* 2014; Zwahlen *et al.* 2017); and selected simulation case studies (Ozah *et al*. 2005; Pickup *et al*. 2011; Pruess & Nordbotten 2011; Sato *et al*. 2011; Bonneville *et al*. 2013; Kempka *et al*. 2014; Orsini *et al*. 2014).

Fig. 4: Fraction of total injected, simulated, or emplaced CO_2 dissolved per year, plotted against total simulation or residence time. The circle areas are scaled to the total mass of CO_2 in each study. A minimum point size is applied to make the position of Pruess & Nordbotten (2011), Sato *et al*. (2011) and Kempka *et al*. (2014) visible. The dashed trend lines represent a log-log gradient for a 10x reduction in average dissolution rate with a corresponding 10x increase in storage time. The high dissolution trend represents 100% of CO_2 dissolving. This is equivalent to 10x the average annual dissolution rate for CO_2 at Sleipner (Alnes *et al.* 2011). The low dissolution trend, representing 10% of CO_2 dissolving, is approximately equivalent to the average annual Sleipner rate.

Fig. 5: Linear time plot of average dissolution rate for all studies excluding the near-field and far-field outliers (Sleipner, Bonneville *et al.* (2013) and 'old' Bravo Dome). When treated as a single population, the exponential trend line has a poor correlation ($R^2 < 0.7$). The coefficient of determination improves ($R^2 > 0.95$) when the case studies are grouped as high and moderate rate populations. At t_0, the high-rate trend is equal to 0.07%, under predicting the average Sleipner rate, 0.9%, by a factor of 13. In the far-field to the right of the plot, at 100 kyr, the bridge point between 'young' and 'old' Bravo Dome models, the fraction of CO_2 dissolved per year has decayed to less than 10^{-10} for all trend lines.

Fig. 6: Dissolution rates over time (**a**) in log-log domain, and (**b**) plotted linearly for the first 5.5 kyr. Note the deviation of Bonneville *et al.* (2013) from a constant log-log gradient, indicating a rapid decline in dissolution within 100 years. For Sathaye *et al.* (2014), both the initial rate to 5 kyr and the long-term rate to 1.2–1.5 Ma are shown. Plotted studies: Sleipner (Alnes *et al*. 2011); Bravo Dome (Sathaye *et al.* 2014; Zwahlen *et al.* 2017). Simulations: Ozah *et al*. 2005; Pruess & Nordbotten 2011; Sato *et al*. 2011; Bonneville *et al*. 2013; Kempka *et al*. 2014. Analytical: Szulczewski *et al*. 2013.

Tables

Table 1: *CO_2 dissolution mass, age and rate estimates for Bravo Dome analogue studies*

Bravo Dome Publications	**Emplaced CO_2 (Mt)**	**Dissolved CO_2 (Mt)**	**Estimated Fraction Dissolved**	**Age of CO_2 emplacement**	**Dissolution rate (Mt/kyr)***
Sathaye *et al*. (2014)	1600 ± 670	366 ± 120	0.11 – 0.52	1.2 – 1.5 Ma	0.3
Zwahlen *et al.* (2017)	1800 ± 670	506 ± 166	0.14 – 0.59	14 – 17 ka	32.6

*Mid-point of age estimates used

Table 2: *Case studies and simulations summary*

Publication	**Approach**	**Location and Setting**	**CO_2 Mass (Mt)**	**Fraction Dissolved**	**Model/CO_2 storage duration (yr)**	**Fraction CO_2 dissolved /yr**
Ozah *et al*. 2005	Simulation - GEM	Generic Gulf Coast saline aquifer, USA	48.0	0.31	10000	3.13×10^{-5}
Pickup *et al*. 2011	Simulation - Eclipse 300	Sherwood Formation, East Irish Sea, UK	225	0.36	7000	5.14×10^{-5}
Pruess & Nordbotten 2011	Simulation - TOUGH2	Generic Continental USA	0.160	0.09	418	2.12×10^{-4}
Sato *et al*. 2011	Simulation - GEM	Nagaoka pilot site; Haizume Formation, Japan	0.010	0.59	1000	5.89×10^{-4}
Bonneville *et al*. 2013	Simulation - STOMP-CO2	Proposed FutureGen 2.0 site; Mt Simon Formation, Illinois, USA	33.0	0.18	100	1.82×10^{-3}

Szulczewski *et al*. 2013	Analytical model	Generic aquifer	3214*		10000000	1.00 x-10^{-7}
Kempka *et al*. 2014	Simulation - ECLIPSE100	Ketzin pilot site; Stuttgart Formation, Germany	0.067	0.89	10000	8.92 x 10^{-5}
Orsini *et al*. 2014	Simulation - PFLOWTRAN	Carbonate aquifer, offshore Italy	30.0	0.79	2000	3.95 x 10^{-4}
Alnes *et al*. 2011	Gravimetric survey	Sleipner pilot site, Utsira Formation, North Sea, Norway	11.3	0.13	13	9.69 x 10^{-3}
Sathaye *et al*. 2014	Isotope geochemistry	Bravo Dome, New Mexico, USA	1600	0.23	1350000	1.69 x 10^{-7}
Zwahlen *et al*. 2017	Isotope geochemistry	Bravo Dome, New Mexico, USA	1800	0.28	15500	1.81 x 10^{-5}

*Model uses constant supply of CO_2 above the reservoir. The CO_2 mass value is equal to the mass of CO_2 dissolved into the reservoir

Figure 1

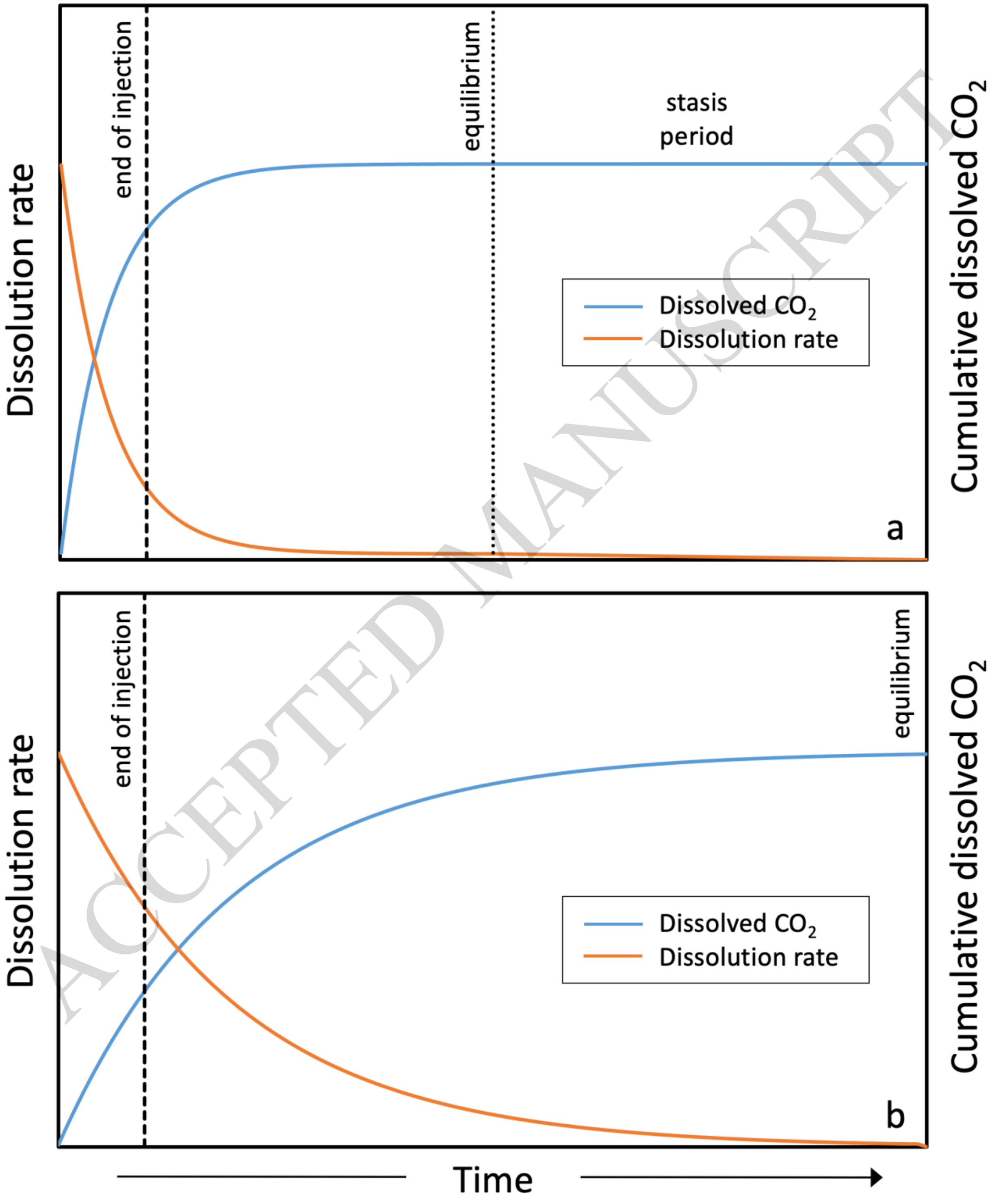

Dissolution rate
end of injection
equilibrium
stasis
period
Cumulative dissolved CO$_2$
Dissolved CO$_2$
Dissolution rate
a
Dissolution rate
end of injection
equilibrium
Cumulative dissolved CO$_2$
Dissolved CO$_2$
Dissolution rate
b
Time

Figure 2

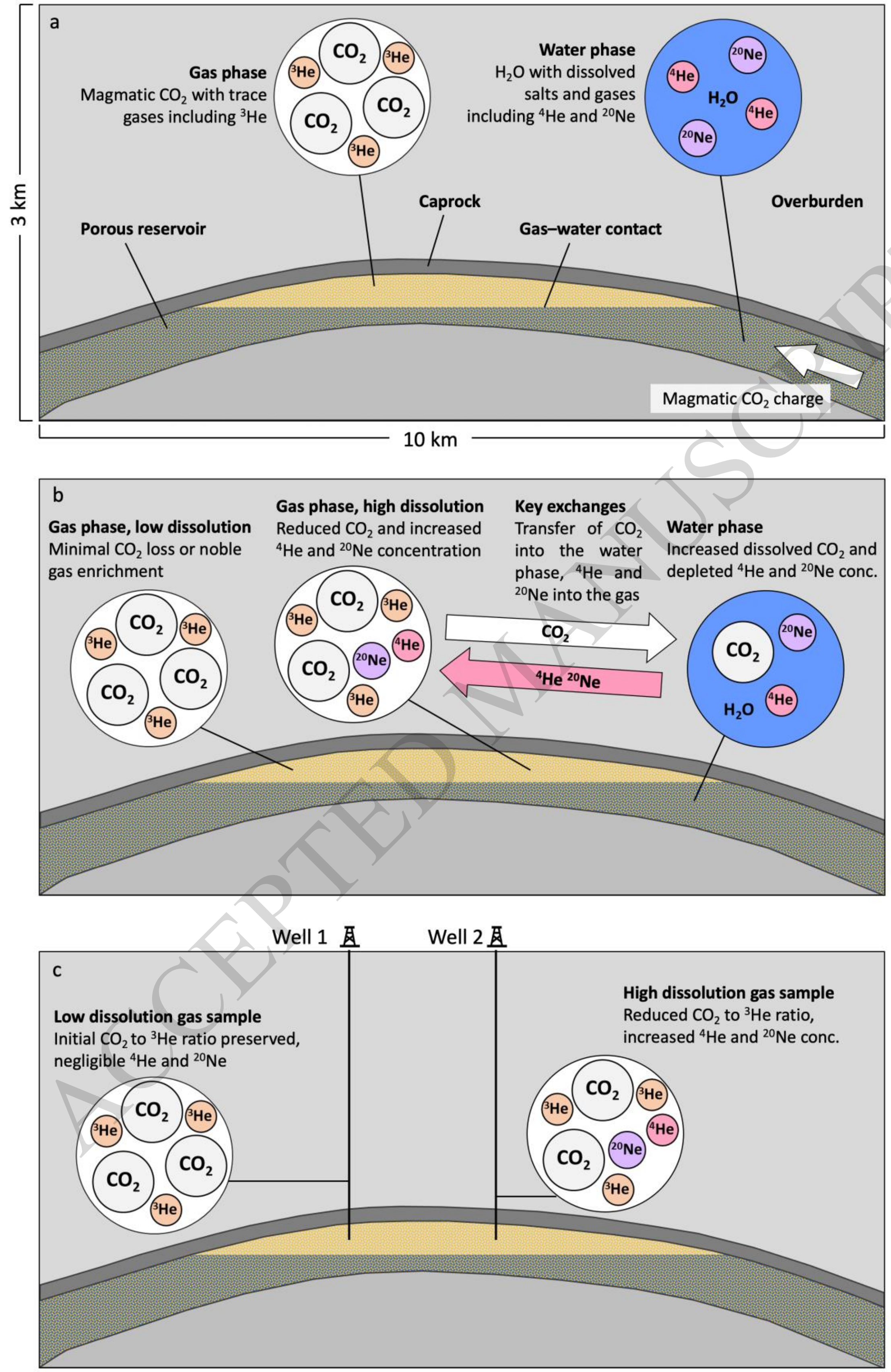

a
Gas phase
Magmatic CO_2 with trace gases including ^3He
CO_2
^3He
Water phase
H_2O with dissolved salts and gases including ^4He and ^{20}Ne
H_2O
^4He
^{20}Ne
Caprock
Overburden
Porous reservoir
Gas–water contact
Magmatic CO_2 charge
3 km
10 km
b
Gas phase, low dissolution
Minimal CO_2 loss or noble gas enrichment
Gas phase, high dissolution
Reduced CO_2 and increased ^4He and ^{20}Ne concentration
Key exchanges
Transfer of CO_2 into the water phase, ^4He and ^{20}Ne into the gas
Water phase
Increased dissolved CO_2 and depleted ^4He and ^{20}Ne conc.
CO_2
^4He ^{20}Ne
H_2O
Well 1
Well 2
c
Low dissolution gas sample
Initial CO_2 to ^3He ratio preserved, negligible ^4He and ^{20}Ne
High dissolution gas sample
Reduced CO_2 to ^3He ratio, increased ^4He and ^{20}Ne conc.

Figure 3

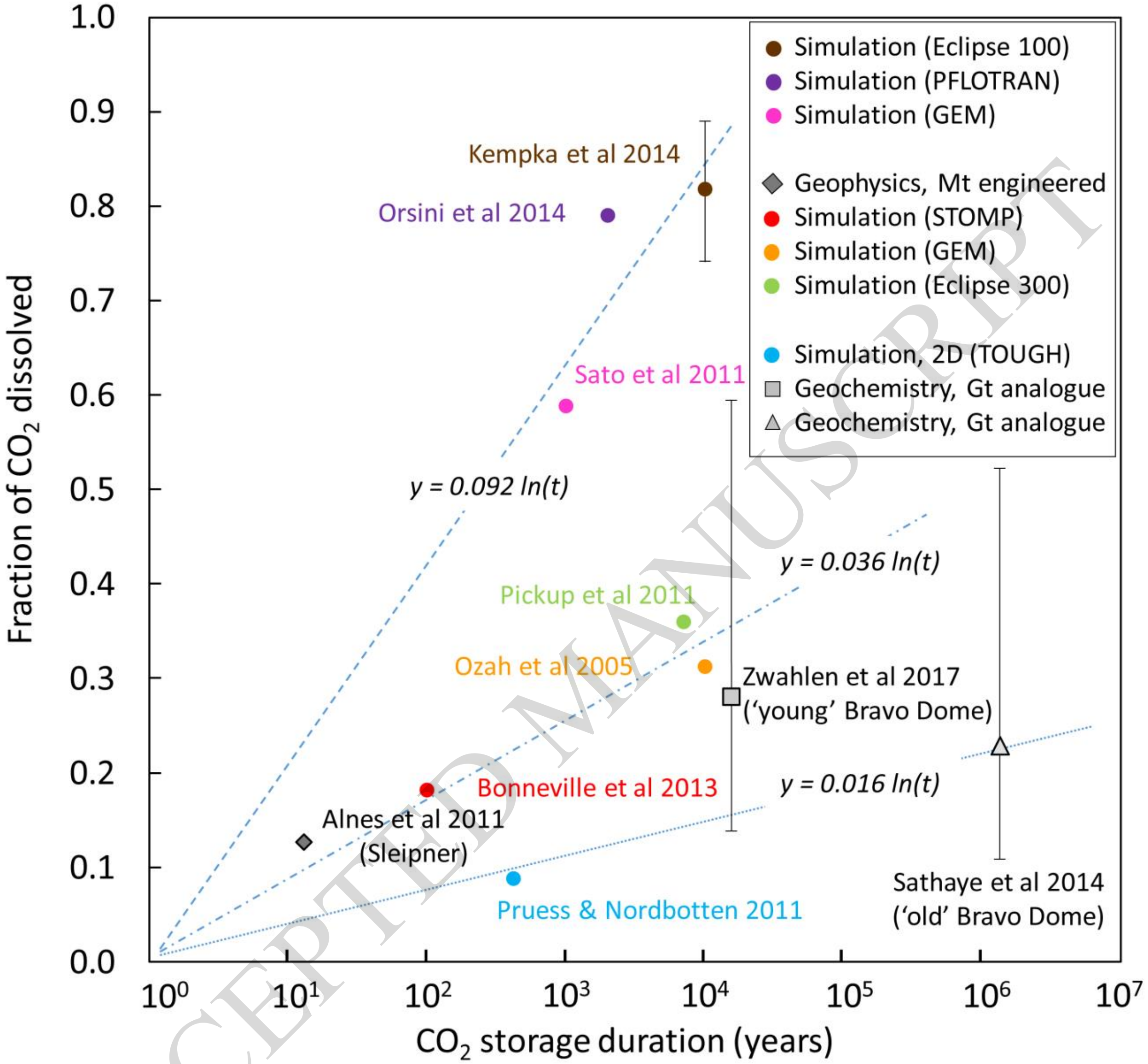

1.0
0.9
0.8
0.7
0.6
0.5
0.4
0.3
0.2
0.1
0.0
Fraction of CO$_2$ dissolved
10^0
10^1
10^2
10^3
10^4
10^5
10^6
10^7
CO$_2$ storage duration (years)
● Simulation (Eclipse 100)
● Simulation (PFLOTRAN)
● Simulation (GEM)
◆ Geophysics, Mt engineered
● Simulation (STOMP)
● Simulation (GEM)
● Simulation (Eclipse 300)
● Simulation, 2D (TOUGH)
■ Geochemistry, Gt analogue
▲ Geochemistry, Gt analogue
Kempka et al 2014
Orsini et al 2014
Sato et al 2011
y = 0.092 ln(t)
y = 0.036 ln(t)
Pickup et al 2011
Ozah et al 2005
Zwahlen et al 2017
('young' Bravo Dome)
Bonneville et al 2013
y = 0.016 ln(t)
Alnes et al 2011
(Sleipner)
Pruess & Nordbotten 2011
Sathaye et al 2014
('old' Bravo Dome)

Figure 4

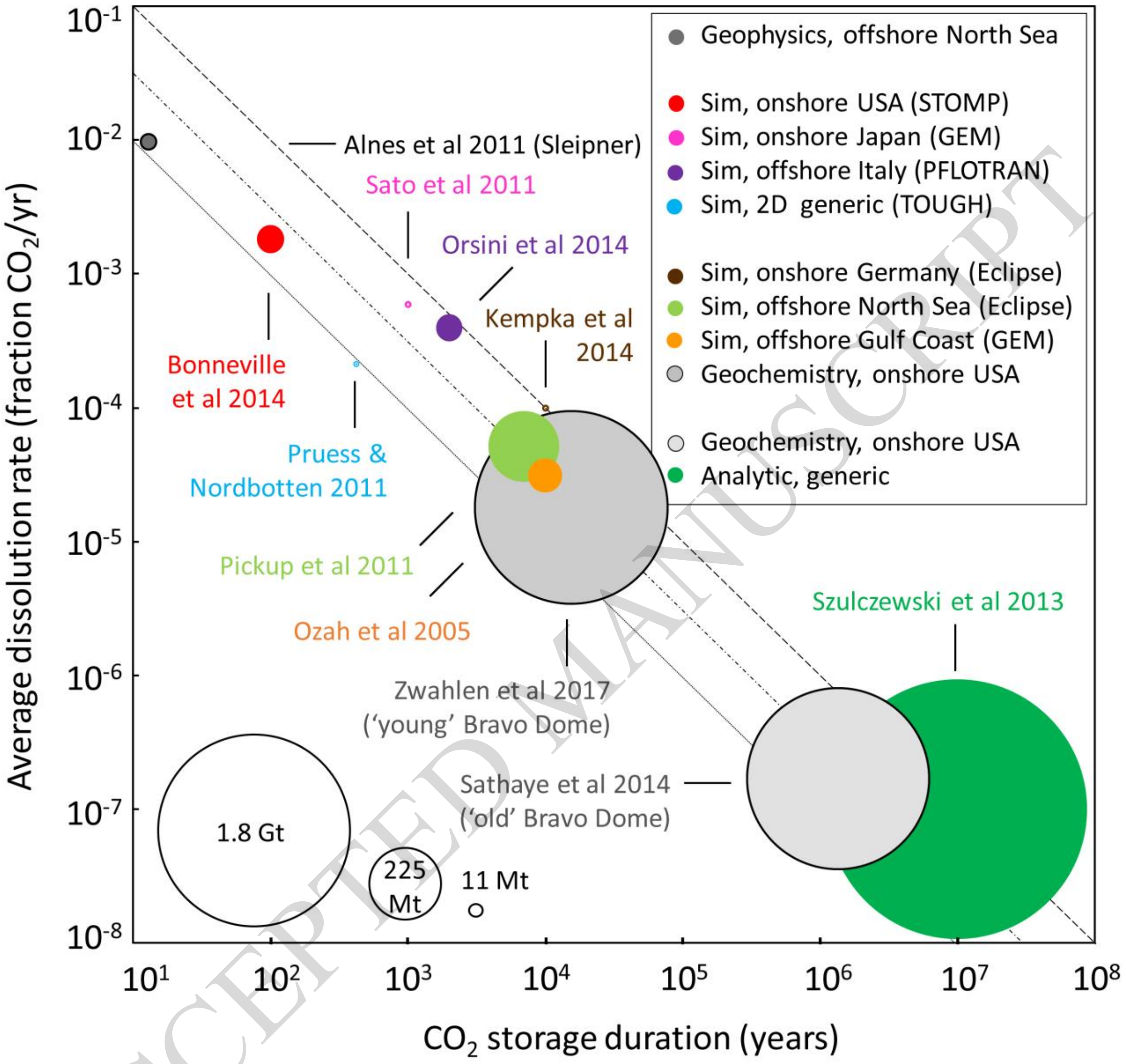

● Geophysics, offshore North Sea
● Sim, onshore USA (STOMP)
● Sim, onshore Japan (GEM)
● Sim, offshore Italy (PFLOTRAN)
● Sim, 2D generic (TOUGH)
● Sim, onshore Germany (Eclipse)
● Sim, offshore North Sea (Eclipse)
● Sim, offshore Gulf Coast (GEM)
● Geochemistry, onshore USA
○ Geochemistry, onshore USA
● Analytic, generic
Alnes et al 2011 (Sleipner)
Sato et al 2011
Orsini et al 2014
Kempka et al 2014
Bonneville et al 2014
Pruess & Nordbotten 2011
Pickup et al 2011
Ozah et al 2005
Zwahlen et al 2017 ('young' Bravo Dome)
Sathaye et al 2014 ('old' Bravo Dome)
Szulczewski et al 2013
1.8 Gt
225 Mt
11 Mt
10^{-1}
10^{-2}
10^{-3}
10^{-4}
10^{-5}
10^{-6}
10^{-7}
10^{-8}
10^1
10^2
10^3
10^4
10^5
10^6
10^7
10^8
Average dissolution rate (fraction CO_2/yr)
CO_2 storage duration (years)

Figure 5

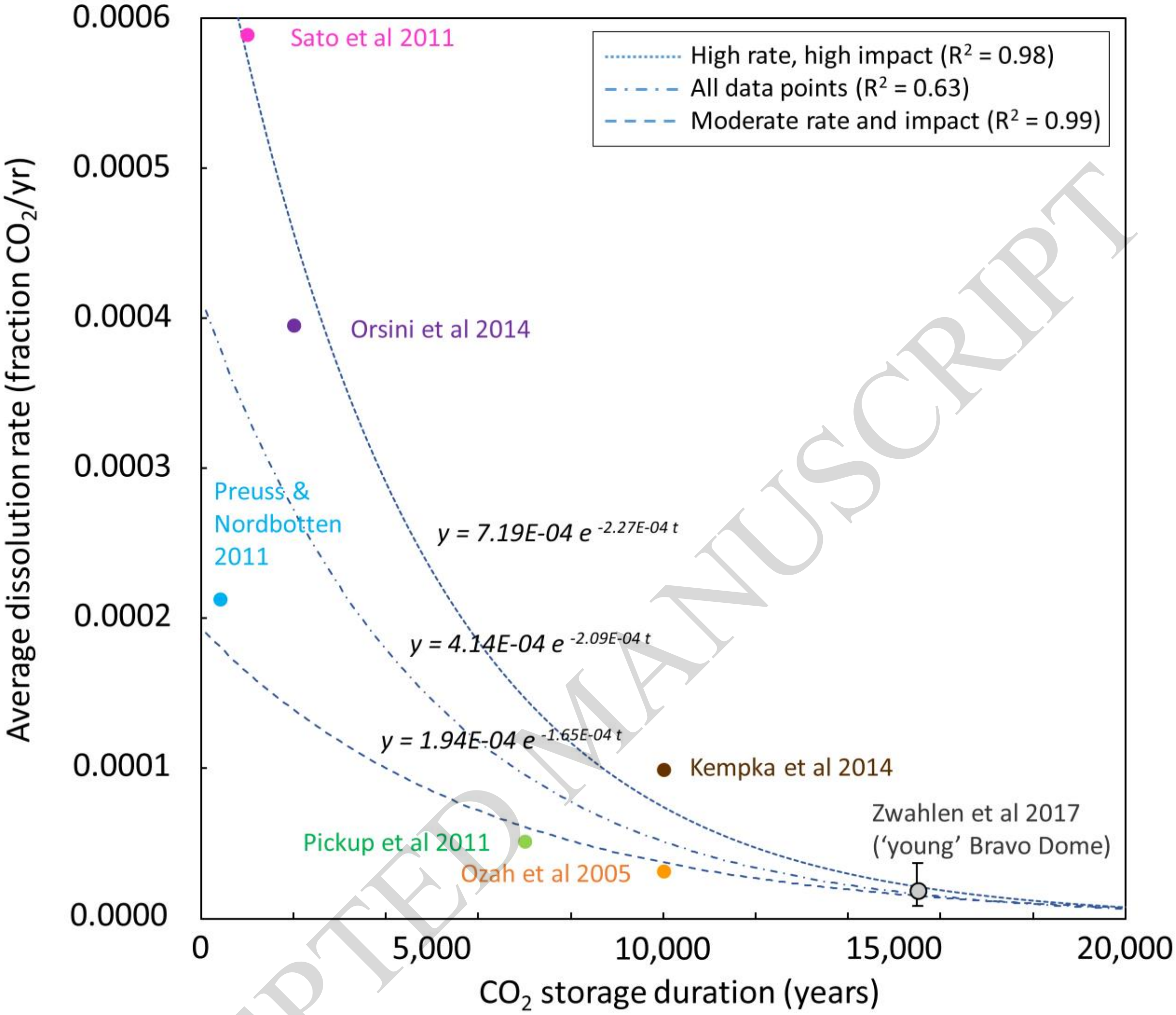
0.0006
0.0005
0.0004
0.0003
0.0002
0.0001
0.0000
Average dissolution rate (fraction CO2/yr)
0
5,000
10,000
15,000
20,000
CO2 storage duration (years)
High rate, high impact (R2 = 0.98)
All data points (R2 = 0.63)
Moderate rate and impact (R2 = 0.99)
Sato et al 2011
Orsini et al 2014
Preuss & Nordbotten 2011
Kempka et al 2014
Pickup et al 2011
Ozah et al 2005
Zwahlen et al 2017 ('young' Bravo Dome)
y = 7.19E-04 e -2.27E-04 t
y = 4.14E-04 e -2.09E-04 t
y = 1.94E-04 e -1.65E-04 t

Figure 6

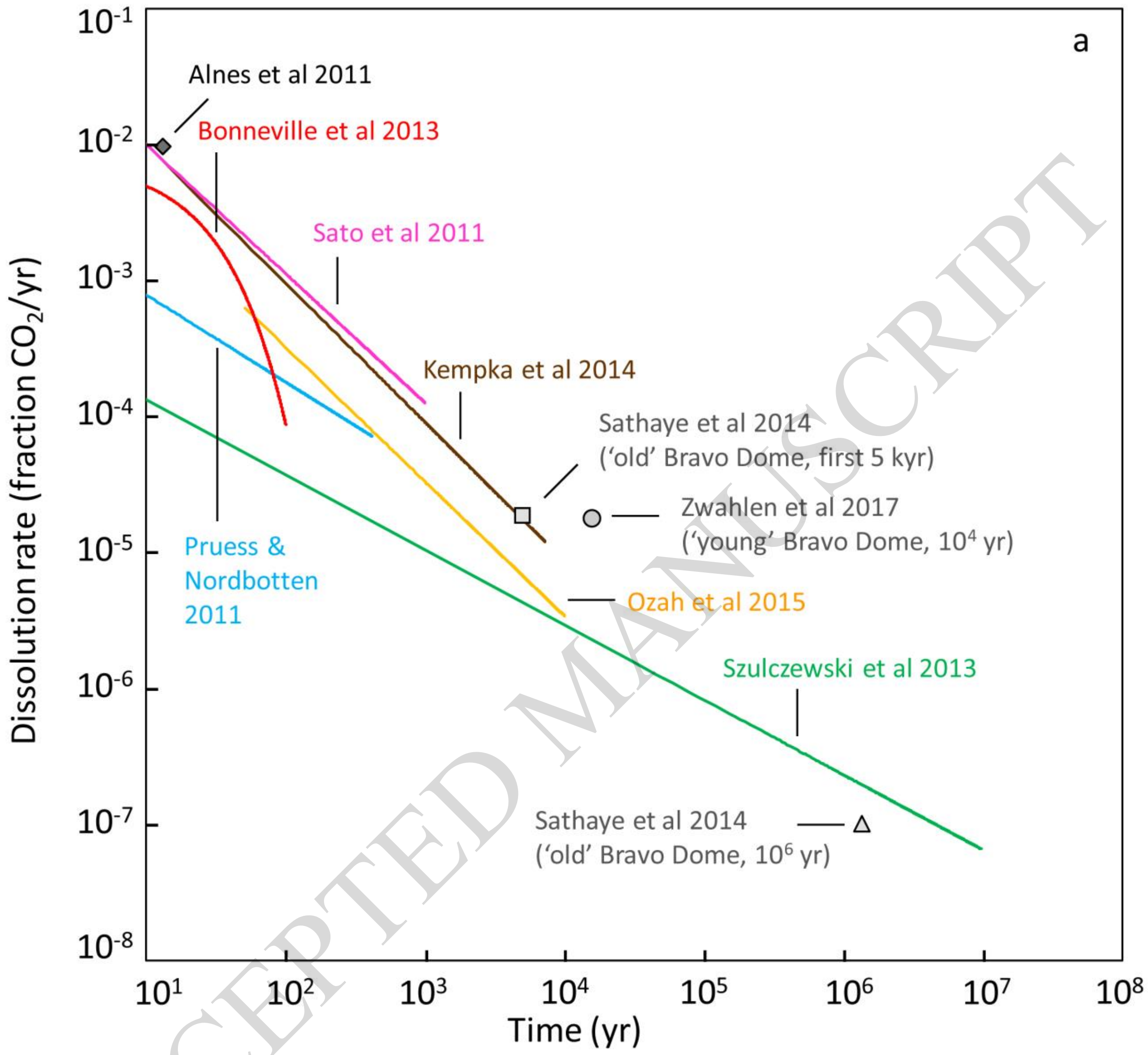
a
Alnes et al 2011
Bonneville et al 2013
Sato et al 2011
Kempka et al 2014
Sathaye et al 2014
('old' Bravo Dome, first 5 kyr)
Zwahlen et al 2017
('young' Bravo Dome, 10^4 yr)
Pruess &
Nordbotten
2011
Ozah et al 2015
Szulczewski et al 2013
Sathaye et al 2014
('old' Bravo Dome, 10^6 yr)
Dissolution rate (fraction CO_2/yr)
10^{-1}
10^{-2}
10^{-3}
10^{-4}
10^{-5}
10^{-6}
10^{-7}
10^{-8}
10^1
10^2
10^3
10^4
10^5
10^6
10^7
10^8
Time (yr)